This is the peer reviewed version of the following article: Tan, P., Chen, B., Xu, H., Cai, W., He, W., Liu, M., ... & Ni, M. (2018). Co3O4 nanosheets as active material for hybrid Zn batteries. Small, 14(21), 1800225, which has been published in final form at https://doi.org/10.1002/smll.201800225. This article may be used for non-commercial purposes in accordance with Wiley Terms and Conditions for Use of Self-Archived Versions.

DOI: 10.1002/ ((please add manuscript number))

Article type: Full Paper

Co₃O₄ Nanosheets as Active Material for Hybrid Zn Batteries

Peng Tan, Bin Chen, Haoran Xu, Weizi Cai, Wei He, Meilin Liu, Zongping Shao*, Meng Ni*

Dr. P. Tan, B. Chen, H. Xu, Dr. W. Cai, Dr. W. He, Prof. M. Ni

Department of Building and Real Estate, The Hong Kong Polytechnic University, Hung Hom, Kowloon, Hong Kong 999077, China

E-mail: bsmengni@polyu.edu.hk

Prof. M. Liu

School of Materials Science and Engineering, Center for Innovative Fuel Cell and Battery Technologies, Georgia Institute of Technology, Atlanta, GA 30332-0245, USA

Prof. Z. Shao

Jiangsu National Synergetic Innovation Center for Advanced Material, College of Energy, State Key Laboratory of Materials-Oriented Chemical Engineering, Nanjing Tech University, Nanjing 210009, China

Email: zongping.shao@curtin.edu.au

Prof. Z. Shao

Department of Chemical Engineering, Curtin University, Perth, WA 6845, Australia

Prof. M. Ni

Environmental Energy Research Group, Research Institute for Sustainable Urban Development (RISUD), The Hong Kong Polytechnic University, Hung Hom, Kowloon, Hong Kong 999077, China

Keywords: cobalt oxide, cycling stability, flexible devices, hybrid Zn battery, working voltage The rapid development of electric vehicles and modern personal electronic devices is severely hindered by the limited energy and power density of the existing power sources. Here a novel hybrid Zn battery is reported which is composed of a nanostructured transition metal oxide-based positive electrode (i.e., Co₃O₄ nanosheets grown on carbon cloth) and a Zn foil negative electrode in an aqueous alkaline electrolyte. The hybrid battery configuration successfully combines the unique advantages of a Zn-Co₃O₄ battery and a Zn-air battery, achieving a high voltage of 1.85 V in the Zn-Co₃O₄ battery region and a high capacity of 792 mAh g_{Zn}⁻¹. In addition, the battery shows high stability while maintaining high energy efficiency (higher than 70%) for over 200 cycle and high rate capabilities. Further, the high flexibility of the carbon cloth substrate allows the construction of a flexible battery with a gel electrolyte, demonstrating not only good rechargeability and stability, but also reasonable mechanical

deformation without noticeable degradation in performance. This work also provides an inspiring example for further explorations of high-performance hybrid and flexible battery systems.

1. Introduction

Metal-air batteries, such as lithium-air, sodium-air, and zinc-air batteries,^[1] are considered promising power sources for a wide range of applications, from personal electronic devices to electric vehicles.^[2] They generate electricity through the electrochemical oxidation of metals by oxygen from ambient air, which neither occupies the volume nor contributes to the weight of the battery. Based on this half-open feature, the theoretical energy densities of metal-air batteries depend largely on the metal electrodes, and have potential to be much higher than those of the state-of-the-art batteries in closed systems.^[3–5] In particular, rechargeable Zn-air batteries have attracted great attention due to their low cost, high safety, and environmental benignity.^[6] However, their practical applications are hindered by a variety of technical hurdles, and one key limitation is the low discharging voltage. Although the theoretical potential can reach 1.65 V, the actual discharging voltage is usually lower than 1.4 V,^[7,8] resulting in low power density and poor rate capability.^[9]

Tremendous efforts have been devoted to improving the discharging voltages of Zn-air batteries, including developing effective catalysts, [10] optimizing electrode structures, [11,12] and designing novel battery configurations. [7,13] However, the standard potential (1.65 V) limits the room for further improvement. Although some Zn batteries in closed systems (e.g., Zn-Ni batteries) can deliver higher working voltages of 1.7 V, [14,15] the theoretical capacities are much lower than that of Zn-air batteries. Hence, the high discharging voltage and large capacity can hardly be achieved simultaneously in any single types of Zn batteries. Recently, a novel concept of hybrid batteries, which combine two sets of different battery reactions at the cell level, has been proposed. [16,17] In addition to oxygen reduction reaction (ORR) and

oxygen evolution reaction (OER) occurring in Zn-air batteries, the redox reactions of transition metal (e.g., MO-OH ↔ MO, M is transition metal) are incorporated to offer a higher voltage. Consequently, higher voltages and more electrochemical energies can be delivered. To realize hybrid Zn batteries, the electrode materials that have high pseudocapacitance and activities toward ORR and OER are crucial. Lee et al. reported NiO/Ni(OH)₂ nanoflakes as the active electrode material for a hybrid Zn battery. [16] With the Faradaic redox reactions of nickel species (Ni³⁺/Ni²⁺) in the Zn-Ni battery region and reversible oxygen reduction and evolution reactions, a high voltage of 1.7 V during initial discharging and a high capacity of 820 mAh g_{Zn}⁻¹ were achieved, and the battery could be cycled over 70 times with stable performance. Li et al. developed an integrated electrode made of NiCo₂O₄ nanowires grown on carbon-coated nickel foam, which enabled a high working voltage (1.7 V) and an excellent stability of over 5000 cycles.^[17] Although active nickel species can provide a high voltage, the phase conversion (i.e., from α -Ni(OH)₂ to β -Ni(OH)₂) in alkaline electrolytes can cause rapid performance degradation. [18,19] Therefore, the exploration of active materials to further improve the battery performance is highly demanded.

Another transition metal, cobalt, has attracted much attention, and cobalt oxides (e.g., CoO, Co₃O₄) have been used as electrocatalysts in various metal-air battery systems, [20–24] due to their facile fabrication, low cost, and high activities. [10] In Zhong's work, Co(OH)₂ and Co₃O₄ nanosheets were in-situ grown on the skeleton of carbon cloth. They found that the apparent overall activity and durability of Co₃O₄ is higher, enabling the Zn-air batteries with low charge-discharge overpotentials (0.67 V), high discharge rate capability (1.18 V at 20 mA cm⁻²), and long cycling stability (400 cycles). [25] Although the intrinsic electrocatalytic activity of Co(OH)₂ is superior, unfortunately, Zn-Co batteries based on Co(OH)₂ can hardly be achieved due to the irreversible issue. [26,27] Recently, a rechargeable Zn-Co₃O₄ battery was reported by Wang et al., which delivered a discharge voltage of 1.78 V, a high energy density

of 241 W h kg⁻¹ (based on the weights of Zn and Co₃O₄), and excellent stability (with capacity retention of 80% after 2000 cycles). ^[28] Inspired by these works, herein we developed a hybrid Zn battery by integrating the electrochemical reactions of Zn-Co₃O₄ and Zn-air batteries through using Co₃O₄ as both active reactant and electrocatalyst. Co₃O₄ nanosheets were in-situ grown on the carbon cloth surfaces to improve the electrical conductivity, and the mesoporous structure facilitated the species transport as well as provided a large surface area for electrode reactions. The electrochemical reactions on the two electrodes are simplified as follows:

Positive electrode:

$$Co_3O_4 + OH^- + H_2O \xrightarrow{Charge} 3CoOOH + e^-$$
 (1)

$$CoOOH + OH^{-} \xrightarrow{Charge} CoO_2 + H_2O + e^{-}$$
 (2)

$$4OH^{-} \xrightarrow{\text{Charge} \atop \text{Discharge}} O_2 + 2H_2O + 4e^{-}$$
 (3)

Negative electrode:

$$Zn(OH)_4^{2-} + 2e^- \xrightarrow{Charge} Zn + 4OH^-$$
 (4)

The rapid kinetics of the redox reactions involving cobalt (Equations 1 and 2) generates a higher working voltage, [28–30] while the oxygen reactions (Equation 3) result in a high capacity. Consequently, a hybrid Zn battery with a liquid alkaline electrolyte perfectly integrated the advantages of a Zn-air battery and a Zn-Co₃O₄ battery and delivered a high voltage of 1.85 V and a high capacity of 792 mAh g_{Zn}⁻¹. It also demonstrated high cycling stability while maintaining energy efficiency higher than 70% for over 200 times (100 h) and high-rate charging and discharging capabilities. Moreover, the flexible carbon cloth substrate also enabled the construction of a gel electrolyte-based flexible hybrid Zn battery to achieve high stabilities under various mechanical deformations.

2. Results and Discussion

Vertical Co₃O₄ nanosheets were grown on carbon cloth (Co₃O₄/carbon cloth) using a cathodic electrochemical deposition process, [27] as schematically illustrated in **Figure 1**a. Subsequently, the Co(OH)₂ was heat treated at 300 °C in air for 2 hours to be fully converted to Co₃O₄,^[31] and the loading was measured to be 2.72 mg cm⁻² (Figure S1, Supporting Information). The morphology of the pristine and Co₃O₄-decorated carbon cloth was characterized using scanning electron microscopy (SEM). As shown in Figure S2 (Supporting Information) and Figure 1b, the carbon cloth retained its structure after the fabrication process, while the surfaces of carbon fibers were uniformly coated with nanosheet arrays (Figures 1c), distinctly different from the morphology of the pristine smooth surface. As seen from a closer view of the SEM image in Figure 1d, these nanosheets were intertwined to form a well-connected network. The transmission electron microscopy (TEM) image in Figure 1e shows that each nanosheet was composed of crystal nanoparticles with mesopores formed (marked in yellow circles) due to the continuous release and loss of H₂O molecules and the volume shrinkage during the calcination process.^[32] As a result, the specific surface area reached 98.78 m² g⁻¹ (Figure S3, Supporting Information), which is about two times higher than that of the pristine carbon cloth (38.62 m² g⁻¹). The measured interplanar spacings of 0.165, 0.202, and 0.244 nm are in good agreement with the standard values of (422), (400), and (311) lattice planes of Co₃O₄, respectively. In addition, the selected-area electron diffraction (SAED) pattern inset coincides with the corresponding diffraction of Co₃O₄ (Figure 1f). The X-ray photoelectron spectroscopy (XPS) and X-ray diffraction (XRD) have been further conducted. Two peaks corresponding to Co 2p_{3/2} (779.9 eV) and Co 2p_{1/2} (794.8 eV) are demonstrated (Figure S4, Supporting Information),^[33] and well indexed XRD peaks are presented (Figure 1e), confirming the characteristic of Co₃O₄. The results indicate that the carbon cloth with the growth of Co₃O₄ nanosheets has been successfully fabricated. The mesoporous structure provides a large specific surface area for electrode reactions and is favorable for rapid transport of oxygen and ions.

The electrochemical activities of the Co₃O₄/carbon cloth were first evaluated in 0.1 M KOH electrolyte, and the results are shown in Figure S5 (Supporting Information). In the ORR region, it exhibits a limiting current density of -17.03 mA cm⁻² and a Tafel slope of 93.9 mV dec⁻¹. The average electron transfer number per oxygen molecule for the ORR is determined to be 3.87 at the potential of 0.3 V (vs. RHE), indicating a four-electron transfer process. In the OER region, it delivers the current density of 10 mA cm⁻² at the potential of 1.56 V (vs. RHE), and a Tafel slope of 88.3 mV dec⁻¹ is possessed. The reversible oxygen electrode property can be assessed by the variance of the operating potential at 10 mA cm⁻² in the OER and the half-wave potential in the ORR ($\Delta E = E_{i=10} - E_{1/2}$,). The Co₃O₄/carbon cloth exhibits a ΔE value of 0.924 V, which surpasses the reported noble metals (e.g., Pt/C, ΔE = 1.0 V; Ir/C, $\Delta E = 1.41$ V) and some bifunctional catalysts (e.g., H-Pt/CaMnO₃, $\Delta E = 1.01$ V), [34,35] demonstrating the high ORR and OER activities. Moreover, it preserves 83.06% of its initial current density at a constant potential of 0.3 V (vs. RHE) for the ORR and exhibits an increased overpotential of 0.013 V at a constant current density of 10 mA cm⁻² for the OER after 400 min, showing the high stability during the electrocatalytic processes. To study the hybridized Zn-Co₃O₄ and Zn-air reactions of the Co₃O₄/carbon cloth electrode, the cyclic voltammetric (CV) test was then carried out in 6 M KOH. As shown in Figure S6 (Supporting Information), in addition to the conventional cathodic ORR and anodic OER current at the potentials of <1.0 or >2.1 V, respectively, the CV curve recorded in ambient air includes three pairs of redox peaks in the range of 1.7 and 2.1 V. The first pair (I_a/I_c) corresponds to the electrochemical transition involving Co(OH)₂/Co₃O₄, while the second (II_a/II_c) and the third pair (III_a/III_c) can be attributed to the conversion of Co₃O₄/CoOOH and CoOOH/CoO₂ species, respectively.^[29,30] These phenomena are different from the reported active materials of NiO/Ni(OH)₂ and NiCo₂O₄, in which only one redox couple (i.e., Ni²⁺/Ni³⁺) is presented. [16,17] Besides, these Faradaic reactions are characterized by rapid ion exchange kinetics, resulting in the high pseudocapacitive currents. Further, the redox reactions occur in

a narrower potential window compared to that of the catalytic oxygen reactions, leading to a higher working discharge voltage. Consequently, the resultant Zn-Co₃O₄ battery working in the oxygen-free condition delivers high discharge voltages up to 1.85 V, good rate capabilities, and a capacity retention of 86.5% after 400 charging-discharging cycles (Figure S7, Supporting Information). Therefore, by coupling this Co₃O₄/carbon cloth electrode with a Zn electrode, the resultant battery will be able to reversibly store and deliver electrochemical energy through the redox reactions of cobalt oxides in the Zn-Co₃O₄ battery and ORR/OER in the Zn-air battery.

The performance of a hybrid Zn battery with this Co₃O₄/carbon cloth electrode was investigated in a homemade battery under the ambient air. The battery structure and the corresponding electrochemical processes during discharging and charging are schematically illustrated in Figure 2a, and the photographs of the battery are shown in Figure S8 (Supporting Information) and Figure 2b. After assembling, an open circuit voltage (OCV) of 1.42 V is demonstrated (Figure 2c), corresponding to the equivalent potential between Zn and O₂ (1.65 V).^[6] In the first discharging process, a smooth and flat voltage plateau at about 1.0 V indicates the ORR process of a typical Zn-air battery. In the subsequent charging process, however, two processes occur, including the evolution of Co_3O_4 ($Co_3O_4 \rightarrow CoOOH \rightarrow CoO_2$) and the OER. Due to the formation of Co⁴⁺ after the charging activation, the OCV increases to 1.91 V. In the following discharging process, interestingly, two voltage plateaus are clearly demonstrated: the first plateau near 1.85 V corresponds to the reduction of cobalt ($CoO_2 \rightarrow$ $CoOOH \rightarrow Co_3O_4$), and the second one at 1.0 V corresponds to the ORR. The chemical valence changes of cobalt were proved by XRD results in Figure S9 (Supporting Information). Hence, the discharging and charging behaviors of both Zn-Co₃O₄ and zinc-air batteries coexist in this hybrid battery. Due to the high voltage of Zn-Co₃O₄ reaction, a single hybrid Zn battery can light up a red light-emitting diode (LED, 1.8 V) as shown in Figure 2b, which cannot be achieved by typical Zn-air batteries.^[7,8] In addition, the polarization curve of this

hybrid Zn battery after the first charging activation shows a high peak power density of 41 mW cm⁻² at 24 mA cm⁻² (Figure S10, Supporting Information), indicating the high power density feature attributed to the rapid kinetics of the Zn-Co₃O₄ battery. After the exhausting of active cobalt species, the galvanostatic discharging performance examined at the current densities of 1, 2, and 5 mA cm⁻² results in the voltage plateaus of 1.15, 1.09, and 0.87 V, respectively, and the specific capacities of 792, 771, 743 mAh g_{Zn}^{-1} , respectively (Figure 2d). The discharging capacities are very close to the theoretical value (820 mAh g_{Zn}^{-1}), highlighting the high capacity feature from the Zn-air battery. On the basis of the weight of Co₃O₄ and consumed Zn, the energy densities are calculated to be 846, 768, 578 W h kg⁻¹, respectively, much higher than that of the reported Zn-Co₃O₄ battery (241 W h kg⁻¹).

The stability of the hybrid battery was investigated by pulse discharging-charging tests at 1 mA cm⁻², and the result is shown in Figure 2e. Initially, the low oxygen concentration in the electrolyte results in the low discharge voltage plateau. With the cycle number increasing, the oxygen concentration gradually increases, improving the discharge voltage plateau.^[1] After the stabilization over several initial cycles, the oxygen concentration in the electrolyte becomes saturated. Thus, stable discharging and charging voltages of 1.15 and 1.98 V over 200 cycles were maintained. The two-step voltage profiles were retained throughout the cycling tests, as illustrated by selected cycles shown in Figure 2f. Attributed to the high voltage of the Zn-Co₃O₄ reaction, the energy efficiency was stable at 71% (Figure S11, Supporting Information), higher than that of conventional Zn-air batteries (Table S2, Supporting Information). Due to the half-open system, carbon dioxide will enter the alkaline electrolyte, decreasing the ionic conductivity. [37] In addition, the evaporation of liquid electrolyte will shrink the reaction boundaries.^[38] Both can increase the discharging and charging overpotentials, affecting the electrochemical performance. To this end, we replaced the electrolyte with a fresh one after 200 cycles (Figure S12, Supporting Information). It is found that another stable 200 cycles with the energy efficiency of around 70% could be

delivered, and both the voltage plateau and the capacity of Zn-Co₃O₄ reaction recovered to some extent (Figure S13, Supporting Information). After cycling, the hybrid Zn battery was dissembled. As shown in Figure S14 (Supporting Information), the electrode structure remained the same, and both the morphology and the crystal structure of Co₃O₄ were maintained, indicating the high stability of the Co₃O₄/carbon cloth electrode. However, zinc dendrite could be clearly witnessed on the Zn foil surface (Figure S15, Supporting Information), which could cause internal short-circuit and threaten the long-time operation safety.^[38] Therefore, suppressing the dendrite formation is one key for the long-term stability of the whole battery.

In addition to the conventional cycling stability test, a high-rate capability of the hybrid Zn battery with this Co₃O₄/carbon cloth electrode was evaluated. To stabilize the high-rate cycling, the battery was firstly cycled at 1 mA cm⁻² for activation (Figure S16, Supporting Information). After that, it was cycled at the charging current densities of 2, 5, 10, and 15 mA cm⁻², respectively, and maintained the discharging current density of 1 mA cm⁻² for a fixed capacity (0.33 mAh cm⁻²). As shown in **Figure 3**a, the charging voltages gradually increase with increasing current density, while the discharging voltages are almost maintained during each cycle. At different charging voltages, it is clear to find that even though the charge current density increases from 2 to 15 mA cm⁻², the discharging voltage profiles and the obtainable capacities for both Zn-Co₃O₄ and Zn-air reactions remain unchanged (Figure 3b). The high-rate discharging capability was further tested through charging at the same current density of 1 mA cm⁻² but discharging at 2, 5, 10, and 15 mA cm⁻², respectively, for a fixed capacity (0.33 mAh cm⁻²). As shown in Figure 3c and 3d, the discharging voltages decreased with increasing current density, especially for the voltage plateau at the Zn-air battery region. While even at high current densities, the two-step voltage profiles were maintained, and the capacity retention of the Zn-Co₃O₄ reaction reached 51.4% when the current density increased 10 times (from 1 to 10 mA cm⁻²) (Figure S17, Supporting Information), higher than the

reported value.^[28] When charging the battery using the same current density (1 mA cm⁻²), the charging voltage plateaus was recovered. Hence, the high-rate tests demonstrated the capability of the hybrid Zn battery in two operation modes: in the fast-charging mode, both the discharging voltage and capacity can be maintained, reducing the charging time; in the fast-discharging mode, a high voltage coming from the Zn-Co₃O₄ reaction can also be delivered, providing a high power for acceleration.

Attributed to the high flexibility of the carbon cloth substrate, [13,22] the Co₃O₄/carbon cloth electrode can be further incorporated into flexible batteries. [39] For a simple proof-ofconcept, we built a flexible hybrid battery, as schematically illustrated in Figure 4a. A gel electrolyte membrane was sandwiched between the Zn foil electrode and the Co₃O₄/carbon cloth electrode. After connecting the two electrodes with current collectors, the breathable tapes were used to pack the components and provide air pathways (Figure S18, Supporting Information). The photograph of the assembled flexible hybrid Zn battery is shown in Figure 4b, from which an OCV of 1.415 V was obtained, close to the value of the liquid electrolytebased hybrid Zn battery (Figure 2c). The stability test was performed by discharging-charging cycling at 1 mA cm⁻² (20 min per cycle), and the results are presented in Figure 4c and Figure 4d. For the first discharging process, one voltage plateau corresponding to ORR was demonstrated. Starting from the second discharging process, the two-step voltage profiles were clearly observed, consistent with the liquid electrolyte-based battery. After several initial cycles, the discharging voltage plateau gradually increases to a stable value of 1.0 V, due to the improved interfaces after initial activations.^[40] More importantly, the discharging and charging voltage profiles exhibited similar shapes (Figure 4d), indicating the good rechargeability and stability (Table S3, Supporting Information). To assess the flexibility, the hybrid Zn battery was bent under different conditions to change the end-to-end distance (Figure S19, Supporting Information).^[41] As shown in Figure 4e, under the flat and different bending conditions, the discharging and charging voltage profiles were almost the same.

Furthermore, one single battery could successfully light up a red LED, and the brightness remained virtually unchanged even at continuous bending and twisting conditions (Movie S1, Supporting Information), highlighting the potential application for flexible and wearable electronic devices. To practically use the solid-state flexible battery, the long-term stability is an important issue. Since the air electrodes are exposed to the atmosphere, the loss of water in the gel electrolyte by evaporation leads to a fast degradation of the ionic conductivity, severely damaging the battery performance.^[14] In addition, CO₂ in ambient air induces the formation of carbonates, which not only reduces the conductivity but also decreases the active surfaces, threatening the stable operation.^[15] Hence, the developments of stable electrodes and solid-state electrolytes, as well as functional membranes that prevent the evaporation of water and the penetration of CO₂, are essential to building a stable solid-state flexible battery with long cycle life,^[7] which will be our research focus following the present work.

To achieve excellent electrochemical performance, one key feature of the electrode is the formation of large reaction boundaries. In this work, mesoporous Co₃O₄ nanosheets are directly grown on the carbon cloth surfaces without additional binders, maintaining the active surface areas and enhancing the electrical conductivity. [42] Further improvements will focus on optimizing the nanoarchitecture (e.g., reducing the nanosheet thickness) to increase the utilization of Co₃O₄ as both active material and electrochemical catalyst (Figure S7, Supporting Information). [28] Besides the electron transport, the reaction boundaries depend on the contact between the reaction species (Figure S20, Supporting Information). For the Faradaic redox reactions occurring in the Zn-Co₃O₄ battery, the Co₃O₄ surface should be well wetted by the electrolyte for the exchange of hydroxide ions. The Co₃O₄/carbon cloth electrode was fabricated through electrodeposition in an aqueous solution (for details see Supporting Information) and exhibited good hydrophilicity (Figure S21, Supporting Information). Consequently, a power density higher than others was demonstrated (Table S1, Supporting Information). For the ORR in the Zn-air battery, it occurs at the triple-phase

boundaries where the solid catalyst, liquid electrolyte, and gaseous oxygen meet. This structure, however, is absent in the present Co₃O₄/carbon cloth electrode (Figure S21, Supporting Information). Oxygen needs to dissolve in the electrolyte first and then participate in the reduction reaction. The sluggish transport kinetics accounts for the low power density after the consumption of active cobalt species and the low voltage plateaus at high current densities (Figure 3c). One solution is treating the surface with water-repellent additives such as polytetrafluoroethylene (PTFE).^[17] As a proof-of-concept, we treated the Co₃O₄/carbon cloth electrode with PTFE, after which the hydrophobicity is improved, creating the gas transport pathways and increasing the triple-phase boundaries. Consequently, the discharge voltage and the power density are improved apparently (Figure S22, Supporting Information). However, the decreased contact boundaries between the electrolyte and the electrode affect the Faradaic redox reactions, leading to a decreased capacity of the Zn-Co₃O₄ battery. Therefore, the balance between the hydrophobic and hydrophilic properties of the electrode should be further optimized in the liquid electrolyte. [1] For the battery using the gel electrolyte, although gas channels for oxygen transport are provided, the reaction boundaries are severely restricted due to the poor wetting property of the "immobilized" electrolyte. [39] Additionally, to ensure the gas channels for the Zn-air battery, the electrode surface cannot be fully covered by the gel electrolyte, which inevitably causes a waste of the active material in the integrated electrode (Figure S20, Supporting Information). The limited reaction boundaries, high ionic resistance, and the low utilization of active Co₃O₄ may cause the decreased discharging voltage plateaus and capacities (Figure 4c). Further study on improving the electrochemical performance is still on-going through careful design of the active material and the electrode structure. Besides, to enable a stable hybrid Zn battery for practical applications, addressing the issues of the Zn electrode, including suppressing the dendrite formation, increasing the zinc utilization, and enhancing the mechanical flexibility and durability, requires more research effort.[38]

3. Conclusions

In summary, we have developed a hybrid Zn battery based on a nanostructured Co₃O₄ electrode in which the unique advantages of two battery systems (Zn-Co₃O₄ and Zn-air) are well utilized. The mesoporous Co₃O₄ nanosheets grown on carbon cloth greatly reduced the interfacial resistance and improved the electrical conductivity. In addition, the highly porous nanoarchitecture provides large surface areas for electrochemical reactions and allows fast transport of oxygen and ions through the electrode system. These features result in excellent electrochemical reversibility and rate capability for the redox reactions involving active cobalt species and for oxygen reduction and evolution reactions. When this Co₃O₄/carbon cloth electrode was incorporated in an aqueous electrolyte-based hybrid Zn battery, it delivered a high voltage of 1.85 V in the Zn-Co₃O₄ battery region. After the consumption of active cobalt species, the behavior of the Zn-air battery was presented, resulting in a high energy density of 792 mAh g_{Zn}⁻¹. Besides, the battery could be continuously discharged and charged for over 200 cycles (100 h) while maintaining an energy efficiency of higher than 70%. Moreover, the high-rate capability was demonstrated at various charging and discharging current densities (ranging from 2 to 15 mA cm⁻²), implying high power density and short charging time. Attributed to the high flexibility of the carbon cloth substrate, a flexible hybrid Zn battery was constructed using a gel electrolyte, which displayed not only good rechargeability and stability, but also reasonable mechanical deformation without noticeable degradation in performance. This work provides inspiration for the explorations of novel active materials for a new generation of high-performance hybrid battery systems for electric vehicles and flexible electronic devices.

4. Experimental Section

Preparation of Co₃O₄ nanosheets on the carbon cloth: A piece of carbon cloth was first heat treated at 500 °C in air for 4 hours to improve its wettability and then rinsed with distilled water and ethanol, respectively. The electrodeposition was performed as reported before.^[31]

Briefly, a standard three-electrode glass cell consisting of the carbon cloth electrode, a platinum counter electrode, and a Hg/HgO reference electrode was used. The Co(OH)₂ was electrodeposited upon carbon cloth in 100 mL of 0.1 M Co(NO₃)₂·6H₂O solution under a potential of –1.0 V (vs. Hg/HgO) using a Solartron SI 1287 potentiostat. After electrodeposition for 30 min, the carbon cloth substrate was taken off, rinsed several times with distilled water and ethanol carefully, and dried in air. After that, the substrate was calcined at 300 °C in air for 2 hours to convert Co(OH)₂ to Co₃O₄.

Physicochemical characterization: The morphologies were observed by a scanning electron microscope (SEM, VEGA3 TESCAN) under an acceleration voltage of 20 kV. Transmission electron microscopy (TEM) images were obtained by operating a high-resolution JEOL 2100F TEM system with a LaB₆ filament at 200 kV. The samples were dispersed in ethanol, sonicated and dripped onto the holey carbon-coated Cu grids. The compositions of the synthesized materials were analyzed by X-ray diffraction (XRD, Rigaku Smartlab) using a Cu-Kα source operating at 40 keV. The X-ray photoelectron spectroscopy (XPS) characterization was determined by a Physical Electronics PHI 5600 multi-technique system using Al monochromatic X-ray at a power of 350 W. The peak position correction was corrected by referencing the C 1s peak position of carbon. The specific surface areas were estimated from the pore-size distribution curves from the desorption isotherms using the Barrett-Joyner-Halenda (BJH) method. The loading of Co₃O₄ grown on the carbon cloth was measured by thermogravimetric analysis (TGA) under the air atmosphere from 50 to 800 °C at a heating rate of 10 °C min⁻¹.

Electrochemical measurements: The electrochemical evaluation was conducted in a standard three-electrode glass cell by rotating disc electrode (RDE) voltammetry using a potentiostat (Solartron SI 1287) and a rotation speed controller (Pine Instrument Co.). The Co₃O₄/carbon cloth with a diameter of 5 mm was fixed on the glassy carbon electrode as the working

electrode. A platinum wire and a Hg/HgO electrode were used as counter and reference electrodes, respectively, and 0.1 M KOH was used as the electrolyte. Pure oxygen gas was purged for 1 h before each RDE experiment to make the electrolyte saturated with oxygen. Linear sweep voltammetry (LSV) for ORR polarization curves was conducted using various rotation speeds (400, 625, 900, 1225, 1600, and 2025 rpm) with at a scan rate of 5 mV s⁻¹ within the potential range from 0.2 to -0.6 V vs. Hg/HgO in the O₂-saturated electrolyte. The kinetic current of electrocatalyst was obtained from mass transfer correction using Koutecky-Levich equation as:

$$j^{-1} = j_k^{-1} + j_d^{-1} \tag{5}$$

where j is the measured current density and j_k and j_d are the kinetic and diffusion-limiting current densities, respectively.

$$j_d = 0.2nFD_{O_2}^{2/3}v^{-1/6}C_{O_2}\omega^{1/2}$$
(6)

where $_{\omega}$ is the angular velocity (rpm), n is the transferred electron number, F is the Faraday constant, $_{D_{o_2}}$ is the diffusion coefficient of O₂ in 0.1 M KOH (1.86 × 10⁵ cm⁻² s⁻¹), $_{v}$ is the kinematic viscosity (1.01 × 10⁻² cm⁻² s⁻¹), and $_{C_{o_2}}$ is the bulk concentration of O₂ (1.21 × 10⁻⁶ mol cm⁻³). LSV for OER polarization curves was conducted using 1600 rpm with at a scan rate of 5 mV s⁻¹ within the potential range from 0.2 to 0.8 V vs. Hg/HgO. All potentials were converted to a reversible hydrogen electrode (RHE) scale via calibration:

$$E_{\text{RHE}} = E_{\text{Hg/HgO}} + 0.059 \text{pH} + 0.098 \tag{7}$$

The electrochemical stability tests of the Co_3O_4 /carbon cloth were carried out at a constant potential of 0.30 V (vs. RHE) for the ORR and at a constant current density of 10 mA cm⁻² for the OER. The cyclic voltammetric (CV) test of the Co_3O_4 /carbon cloth electrode was performed in a three-electrode cell with Zn as both the counter and the reference electrodes. *Fabrication of hybrid Zn batteries:* The conventional Zn battery was composed of the asprepared Co_3O_4 /carbon cloth electrode, a carbon paper as the gas diffusion layer, a Zn foil as

the metal electrode, and 6 M KOH + 0.02 M zinc acetate as the electrolyte. For the polytetrafluoroethylene (PTFE)-treated electrode, the Co₃O₄/carbon cloth was soaked in the 10 wt % PTFE dispersion, drying at 60 °C and then annealed at 300 °C in air for 1 h. To prepare the flexible hybrid Zn battery, a poly(vinyl alcohol) (PVA)-based gel electrolyte was used instead of the liquid electrolyte. 1 g PVA (MW 195000, Aladdin) powder was dissolved in 8 mL distilled water at 80 °C under magnetic stirring. After the solution became transparent, 2 mL of 9 M KOH solution was added and the resultant solution was kept stirring at 80 °C for about 60 min. When the solution became homogenous, a filter paper was fully soaked with the gel electrolyte. After the evaporation of extra water, the filter paper was sandwiched between the Zn foil electrode and the Co₃O₄/carbon cloth electrode. Eventually, both electrodes were connected with the current collectors and sealed by breathable tapes.

Perfromance evaluation of hybrid Zn batteries: To obtained galvanodynamic discharge profiles of the battery, the change in voltage was measured through scaling the current density from 0 to 80 mA cm⁻² at a current step of 1 mA s⁻². To obtain galvanostatic discharge curves, the change in voltage was measured while a fixed current of desired amplitude was applied. The specific capacity (mAh g⁻¹) was calculated according to the consumed zinc during discharge. The charge and discharge cycling was conducted by the same method with a fixed time interval for each state of charge and discharge.

Supporting Information

Supporting Information is available from the Wiley Online Library or from the author.

Conflict of Interest

The authors declare no conflict of interest.

Acknowledgments

M. N. thank the funding support from The Hong Kong Polytechnic University (G-YBJN and G-YW2D), the Environment Conservation Fund (ECF 54/2015) and a fund from RISUD (1-ZVEA).

Received: ((will be filled in by the editorial staff))
Revised: ((will be filled in by the editorial staff))
Published online: ((will be filled in by the editorial staff))

References

- [1] F. Cheng, J. Chen, Chem. Soc. Rev. 2012, 41, 2172.
- [2] Y. Li, J. Lu, ACS Energy Lett. 2017, 2, 1370.
- [3] P. Tan, Z. Wei, W. Shyy, T. S. Zhao, *Appl. Energy* **2013**, *109*, 275.
- [4] K. G. Gallagher, S. Goebel, T. Greszler, M. Mathias, W. Oelerich, D. Eroglu, V. Srinivasan, *Energy Environ. Sci.* 2014, 7, 1555.
- [5] H. Pan, Y. Shao, P. Yan, Y. Cheng, K. S. Han, Z. Nie, C. Wang, J. Yang, X. Li, P. Bhattacharya, K. T. Mueller, J. Liu, *Nat. Energy* 2016, *1*, 16039.
- [6] Y. Li, H. Dai, Chem. Soc. Rev. 2014, 43, 5257.
- [7] Y. Li, M. Gong, Y. Liang, J. Feng, J. E. Kim, H. Wang, G. Hong, B. Zhang, H. Dai, *Nat Commun* **2013**, *4*, 1805.
- [8] J.-I. Jung, M. Risch, S. Park, M. G. Kim, G. Nam, H.-Y. Jeong, Y. Shao-Horn, J. Cho, Energy Environ. Sci. 2016, 9, 176.
- [9] D. U. Lee, P. Xu, Z. P. Cano, A. G. Kashkooli, M. G. Park, Z. Chen, J. Mater. Chem. A 2016, 4, 7107.
- [10] Z.-L. Wang, D. Xu, J.-J. Xu, X.-B. Zhang, Chem. Soc. Rev. 2014, 43, 7746.
- [11] N. Xu, J. Qiao, X. Zhang, C. Ma, S. Jian, Y. Liu, P. Pei, *Appl. Energy* **2016**, *175*, 495.
- [12] J. Fu, F. M. Hassan, J. Li, D. U. Lee, A. R. Ghannoum, G. Lui, M. A. Hoque, Z. Chen, Adv. Mater. 2016, 28, 6421.
- [13] F. Meng, H. Zhong, D. Bao, J. Yan, X. Zhang, J. Am. Chem. Soc. 2016, 138, 10226.
- [14] Y. P. Wu, X. Wang, M. Li, Y. Wang, B. Chen, Y. Zhu, J. Mater. Chem. A 2015, 3, 8280.
- [15] M. Gong, Y. Li, H. Zhang, B. Zhang, W. Zhou, J. Feng, H. Wang, Y. Liang, Z. Fan, J. Liu, H. Dai, Energy Environ. Sci. 2014, 7, 2025.

- [16] D. U. Lee, J. Fu, M. G. Park, H. Liu, A. Ghorbani Kashkooli, Z. Chen, *Nano Lett.* **2016**, 16, 1794.
- [17] B. Li, J. Quan, A. Loh, J. Chai, Y. Chen, C. Tan, X. Ge, T. S. A. Hor, Z. Liu, H. Zhang, Y. Zong, *Nano Lett.* 2017, 17, 156.
- [18] H. Wang, Z. Tamg, Y. Liu, C. Lee, Trans. Nonferrous Met. Soc. China 2009, 19, 170.
- [19] X. Kong, J. Zhao, W. Shi, Y. Zhao, M. Shao, M. Wei, L. Wang, X. Duan, *Electrochim*. Acta 2012, 80, 257.
- [20] D. U. Lee, J.-Y. Choi, K. Feng, H. W. Park, Z. Chen, Adv. Energy Mater. 2014, 4, 1301389.
- [21] X. Chen, B. Liu, C. Zhong, Z. Liu, J. Liu, L. Ma, Y. Deng, X. Han, T. Wu, W. Hu, J. Lu, *Adv. Energy Mater.* **2017**, *7*, 1700779.
- [22] M. Yu, Z. Wang, C. Hou, Z. Wang, C. Liang, C. Zhao, Y. Tong, X. Lu, S. Yang, Adv. Mater. 2017, 29, 1602868.
- [23] Y. Hao, Y. Xu, N. Han, J. Liu, X. Sun, J. Mater. Chem. A 2017, 5, 17804.
- [24] B. Li, X. Ge, F. W. T. Goh, T. S. A. Hor, D. Geng, G. Du, Z. Liu, J. Zhang, X. Liu, Y. Zong, *Nanoscale* 2015, 7, 1830.
- [25] Z. Song, X. Han, Y. Deng, N. Zhao, W. Hu, C. Zhong, ACS Appl. Mater. Interfaces 2017, 9, 22694.
- [26] J. A. Koza, C. M. Hull, Y.-C. Liu, J. A. Switzer, *Chem. Mater.* **2013**, 25, 1922.
- [27] Z. Song, X. Han, Y. Deng, N. Zhao, W. Hu, C. Zhong, ACS Appl. Mater. Interfaces 2017, 9, 22694.
- [28] X. Wang, F. Wang, L. Wang, M. Li, Y. Wang, B. Chen, Y. Zhu, L. Fu, L. Zha, L. Zhang, Y. Wu, W. Huang, Adv. Mater. 2016, 28, 4904.
- [29] I. G. Casella, M. Gatta, J. Electroanal. Chem. 2002, 534, 31.
- [30] P. Nkeng, G. Poillerat, J. F. Koenig, P. Chartier, J. Electrochem. Soc. 1995, 142, 1777.
- [31] L. Huang, D. Chen, Y. Ding, Z. L. Wang, Z. Zeng, M. Liu, ACS Appl. Mater. Interfaces

- **2013**, *5*, 11159.
- [32] Z. Zhu, J. Ping, X. Huang, J. Hu, Q. Chen, X. Ji, C. E. Banks, J. Mater. Sci. 2012, 47, 503.
- [33] A. Younis, D. Chu, X. Lin, J. Lee, S. Li, Nanoscale Res. Lett. 2013, 8, 36.
- [34] A. Aijaz, J. Masa, C. Rösler, W. Xia, P. Weide, A. J. R. Botz, R. A. Fischer, W. Schuhmann, M. Muhler, *Angew. Chemie Int. Ed.* **2016**, *55*, 4087.
- [35] X. Han, F. Cheng, T. Zhang, J. Yang, Y. Hu, J. Chen, Adv. Mater. 2014, 26, 2047.
- [36] J. S. Lee, S. T. Kim, R. Cao, N. S. Choi, M. Liu, K. T. Lee, J. Cho, Adv. Energy Mater.2011, 1, 34.
- [37] J. Fu, J. Zhang, X. Song, H. Zarrin, X. Tian, J. Qiao, L. Rasen, K. Li, Z. Chen, *Energy Environ. Sci.* **2016**, *9*, 663.
- [38] J. Fu, Z. P. Cano, M. G. Park, A. Yu, M. Fowler, Z. Chen, *Adv. Mater.* **2017**, *29*, 1604685.
- [39] P. Tan, B. Chen, H. Xu, H. Zhang, W. Cai, M. Ni, M. Liu, Z. Shao, *Energy Environ. Sci.* 2017, 10, 2056.
- [40] C.-Y. Su, H. Cheng, W. Li, Z.-Q. Liu, N. Li, Z. Hou, F.-Q. Bai, H.-X. Zhang, T.-Y. Ma, *Adv. Energy Mater.* **2017**, *7*, 1602420.
- [41] L. Mao, Q. Meng, A. Ahmad, Z. Wei, Adv. Energy Mater. 2017, 7, 1700535.
- [42] P. Tan, W. Shyy, T. S. Zhao, X. B. Zhu, Z. H. Wei, J. Mater. Chem. A 2015, 3, 19042.

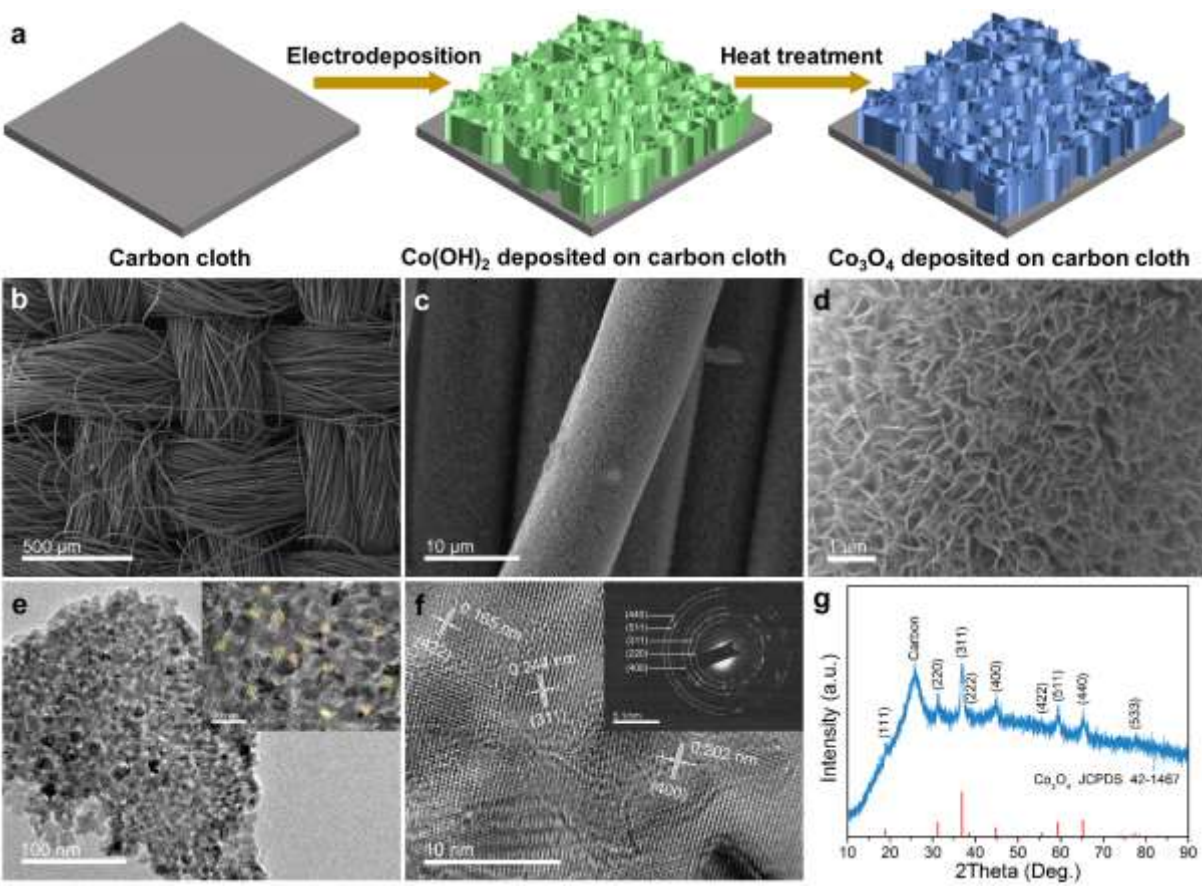


Figure 1. Synthetic procedure and structure characterization of Co_3O_4 nanosheets grown on carbon cloth. a) Schematic of synthesis processes of the Co_3O_4 /carbon cloth composite. b) Low-magnification, c) medium-magnification and d) high-magnification SEM images of Co_3O_4 /carbon cloth. e) TEM image of a Co_3O_4 nanosheet. The inset shows the high-magnification TEM image, the pores formed by nanoparticles are marked in yellow circles. f) High-magnification TEM image of the Co_3O_4 nanoparticles. The inset shows the SAED pattern. g) XRD patterns of the Co_3O_4 /carbon cloth, together with the standard pattern of Co_3O_4 (JCPDS 42-1467).

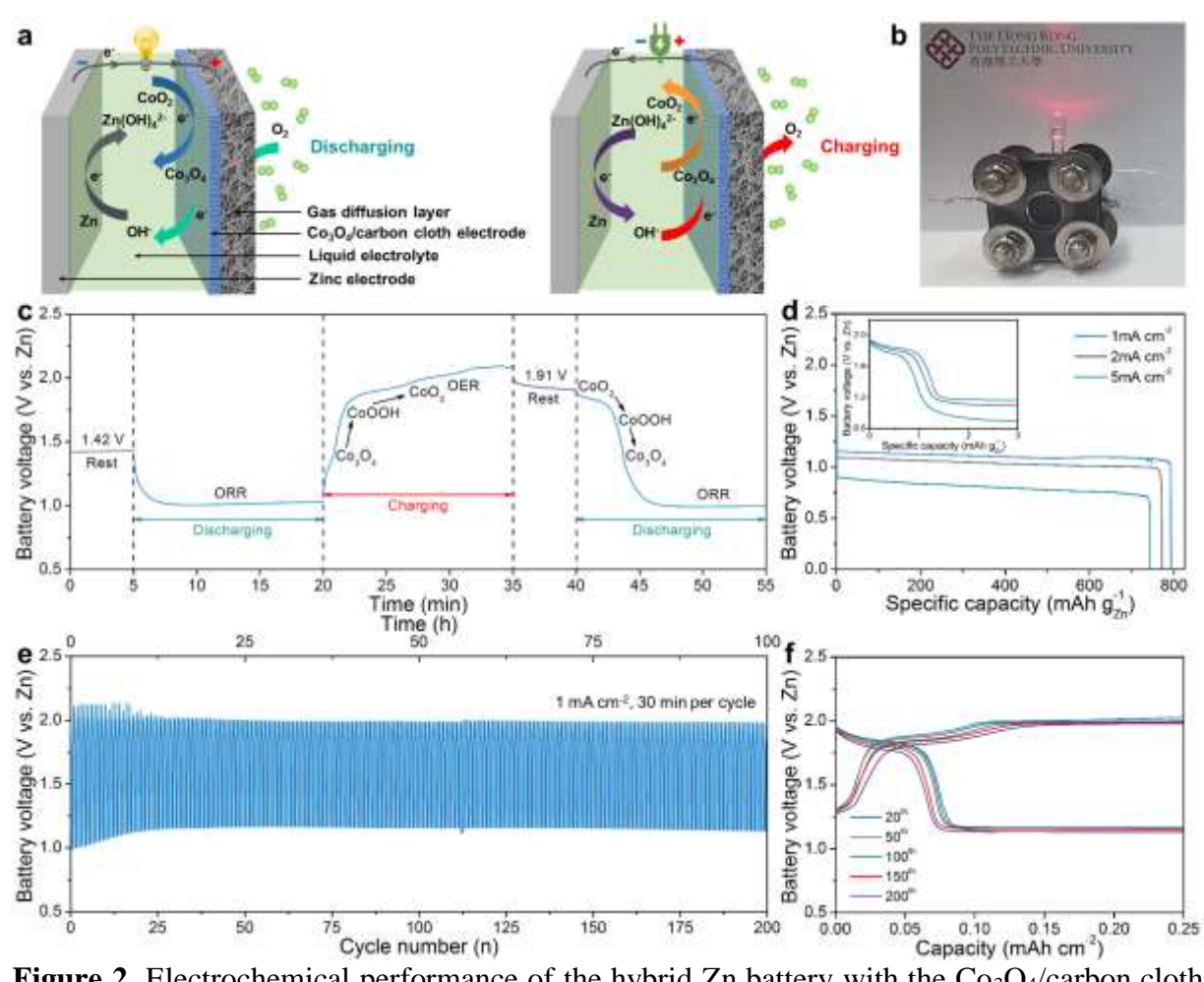


Figure 2. Electrochemical performance of the hybrid Zn battery with the Co₃O₄/carbon cloth electrode based on the liquid electrolyte. a) Schematic illustration of the hybrid Zn battery with the designed electrochemical processes during discharging and charging. b) Photograph of the home-made hybrid Zn battery, a red LED (1.8 V) can be lighted up after the first discharging-charging activation. c) Initial discharging-charging-discharging voltage profiles at 1 mA cm⁻² (15 min for discharging and 15 min for charging). d) Full discharge voltage profiles at current densities of 1, 2, and 5 mA cm⁻² after the discharging-charging activation. Inset: the voltage profiles of Zn-Co₃O₄ Reaction. e) Long-term cycling stability at 1 mA cm⁻² (30 min per cycle). f) Discharging-charging voltage profiles of the 20th, 50th, 100th, 150th, and 200th cycle.

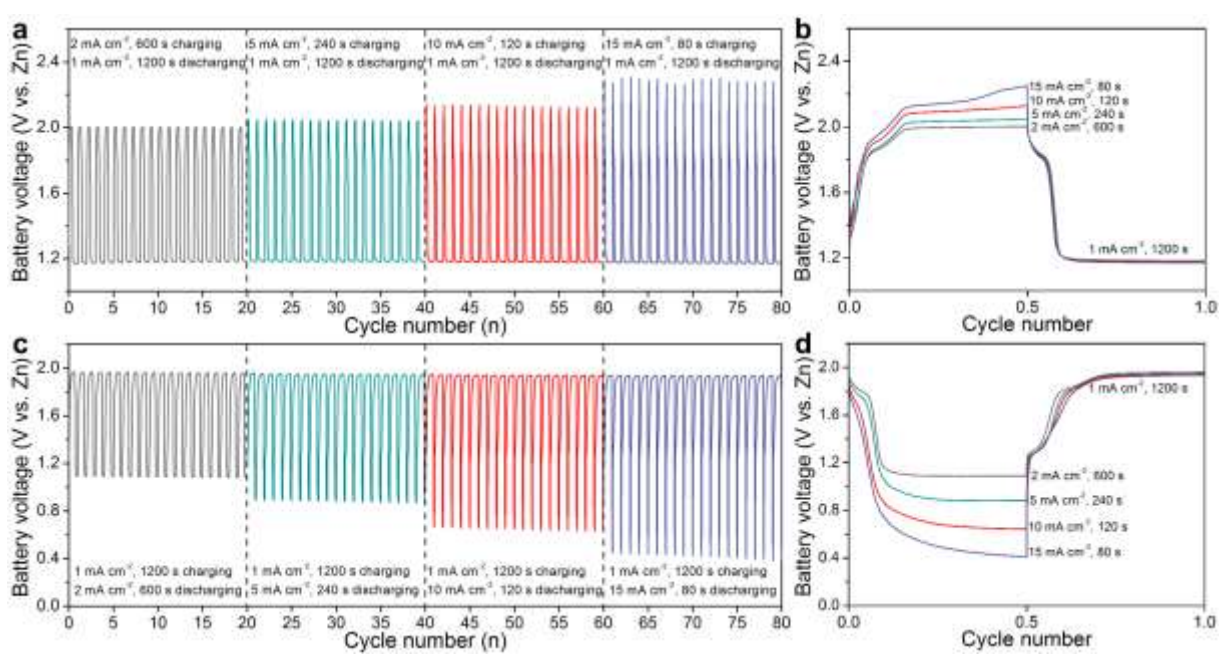


Figure 3. High-rate capability of the hybrid Zn battery with the Co₃O₄/carbon cloth electrode based on a liquid electrolyte. a) Cycling stability test at high charging current densities of 2, 5, 10, and 15 mA cm⁻², respectively, and a discharging current density of 1 mA cm⁻². b) Discharging-charging voltage profiles at different charging current densities at the 10th cycle. c) Cycling stability test at high discharging current densities of 2, 5, 10, and 15 mA cm⁻², respectively, and a charging current density of 1 mA cm⁻². d) Discharging-charging voltage profiles at different discharging current densities at the 10th cycle.

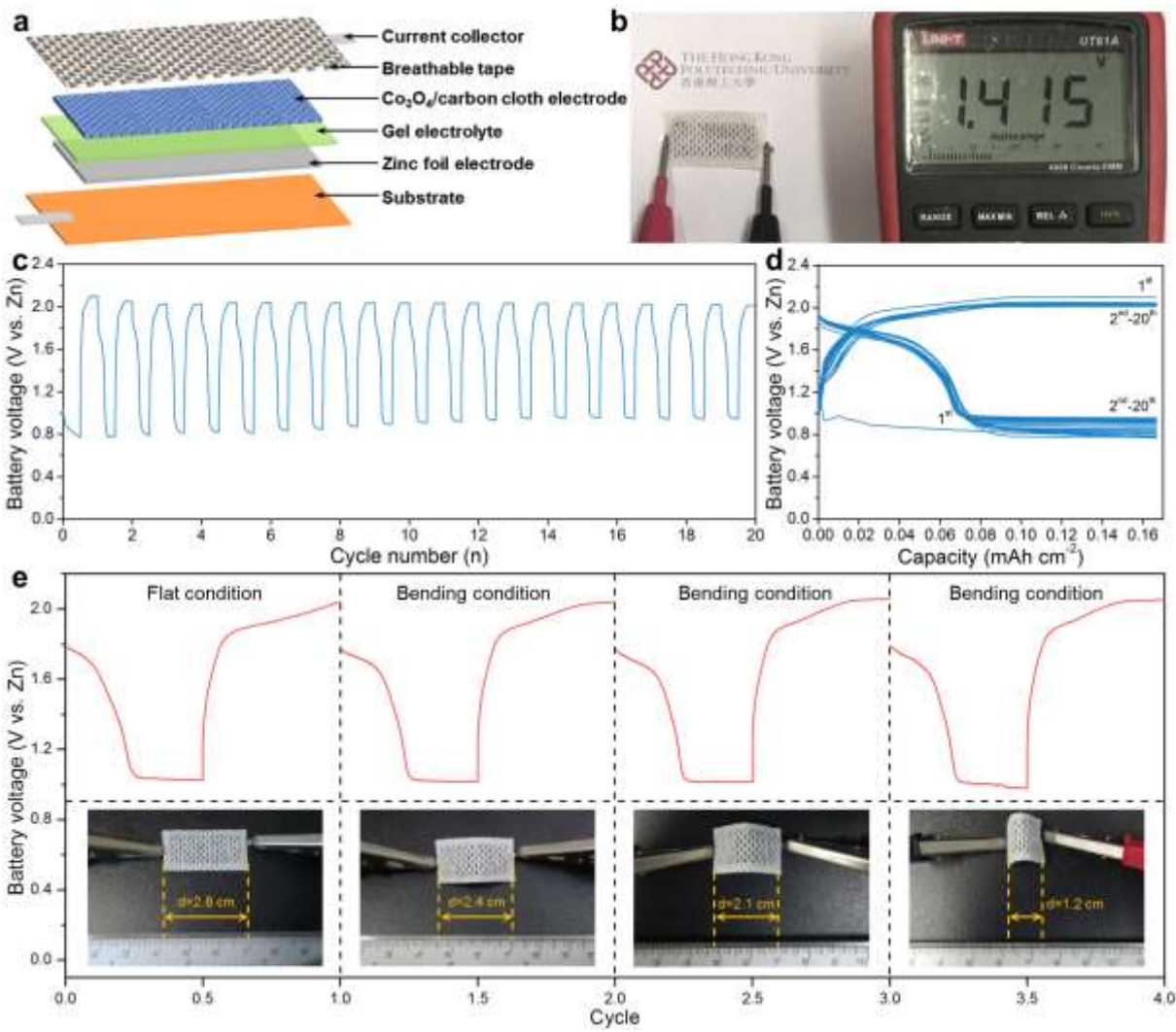


Figure 4. Electrochemical performance of the flexible hybrid Zn battery with the Co₃O₄/carbon cloth electrode based on a gel electrolyte. a) Schematic illustration of the structure of the flexible hybrid Zn battery. b) Photograph of the flexible hybrid Zn battery, an open circuit voltage of 1.4 V is demonstrated after assembling. c) Cycling stability and d) specific capacity at 1 mA cm⁻² (20 min per cycle) as a function of cycle number. e) Discharging-charging voltage profiles at 0.6 mA cm⁻² (10 min for discharging and 10 min for charging) at the flat condition and different bending conditions.

A hybrid Zn battery based on nanostructured Co₃O₄ is developed, in which two different electrochemical reactions of Zn-Co₃O₄ and Zn-air batteries are combined. With the merits of high working voltage, capacity, and cycling stability, such hybrid batteries incorporated with both liquid and gel electrolytes promise high potential for practical applications.

Keyword cobalt oxide, cycling stability, flexible devices, hybrid Zn battery, working voltage

Peng Tan, Bin Chen, Haoran Xu, Weizi Cai, Wei He, Meilin Liu, Zongping Shao*, Meng Ni*

Co₃O₄ Nanosheets as Active Material for Hybrid Zn Batteries

